

Analysis of Coulomb and Johnsen-Rahbek electrostatic chuck performance for extreme ultraviolet lithography

M. R. Sogard, A. R. Mikkelsen, M. Nataraju, K. T. Turner, and R. L. Engelstad

Citation: *Journal of Vacuum Science & Technology B: Microelectronics and Nanometer Structures Processing, Measurement, and Phenomena* **25**, 2155 (2007); doi: 10.1116/1.2798724

View online: <https://doi.org/10.1116/1.2798724>

View Table of Contents: <https://avs.scitation.org/toc/jvn/25/6>

Published by the [American Institute of Physics](#)

ARTICLES YOU MAY BE INTERESTED IN

[Wafer dependence of Johnsen–Rahbek type electrostatic chuck for semiconductor processes](#)

Journal of Applied Physics **102**, 064901 (2007); <https://doi.org/10.1063/1.2778633>

[Generation mechanism of residual clamping force in a bipolar electrostatic chuck](#)

Journal of Vacuum Science & Technology B: Microelectronics and Nanometer Structures Processing, Measurement, and Phenomena **21**, 2371 (2003); <https://doi.org/10.1116/1.1620517>

[Prediction of clamping pressure in a Johnsen-Rahbek-type electrostatic chuck based on circuit simulation](#)

Journal of Vacuum Science & Technology B: Microelectronics and Nanometer Structures Processing, Measurement, and Phenomena **24**, 216 (2006); <https://doi.org/10.1116/1.2151219>

[Effect of wafer bow on electrostatic chucking and back side gas cooling](#)

Journal of Applied Physics **104**, 124902 (2008); <https://doi.org/10.1063/1.3043843>

[Manufacturing issues of electrostatic chucks](#)

Journal of Vacuum Science & Technology B: Microelectronics and Nanometer Structures Processing, Measurement, and Phenomena **13**, 1910 (1995); <https://doi.org/10.1116/1.588108>

[Characterization, modeling, and design of an electrostatic chuck with improved wafer temperature uniformity](#)

Review of Scientific Instruments **66**, 1108 (1995); <https://doi.org/10.1063/1.1145988>

Analysis of Coulomb and Johnsen-Rahbek electrostatic chuck performance for extreme ultraviolet lithography

M. R. Sogard

Nikon Research Corporation of America, Belmont, California 94002

A. R. Mikkelsen,^{a)} M. Nataraju, K. T. Turner, and R. L. Engelstad

Computational Mechanics Center, University of Wisconsin—Madison, Madison, Wisconsin 53706-1572

(Received 9 June 2007; accepted 17 September 2007; published 7 December 2007)

The successful implementation of extreme ultraviolet lithography (EUVL) requires the use of an electrostatic chuck to both support and flatten the mask during scanning exposure. The EUVL Mask and Chucking Standards, SEMI P37 and P40, specify the nonflatness of the mask frontside and backside, as well as the chucking surface, to be on the order of 50 nm peak-to-valley. Thus, characterizing and predicting the capability of the electrostatic chuck to reduce mask nonflatness to meet this specification are critical issues. Details describing the performance of the Coulomb electrostatic chuck have been presented in earlier publications. In this paper, the governing equation identifying the force-gap relationship for a Johnsen-Rahbek (J-R) chuck is described and compared to the Coulomb response. Using finite element techniques, numerical models of Coulomb and J-R electrostatic chucks have been constructed and evaluated for their clamping performance. The models include the effects of reticle and chuck nonflatness, surface friction, and the finite stiffness of the chuck. Modeling predictions are presented for the two types of chucks. The simulations indicate that using a reticle and chuck (Coulomb or J-R style) that meet the SEMI standards for flatness can result in a clamped reticle flatness of less than 100 nm. However, there may be a need to increase the chuck stiffness specified in SEMI P40. These results, which provide the first comprehensive comparison of Coulomb and J-R chucks, are currently being used to establish specifications for chuck geometry and to identify the range of flatness variations that can be accommodated with electrostatic chucking. © 2007 American Vacuum Society.

[DOI: 10.1116/1.2798724]

I. INTRODUCTION

The imaging system in extreme ultraviolet lithography (EUVL) incorporates a reflective mask that is subjected to non-telecentric illumination during exposure. As a result, any nonflatness (i.e., variation of the height) of the pattern surface results in image placement errors on the device wafer. For this reason, it is imperative that the frontside and backside of the reticle, as well as the electrostatic chuck (ESC), be exceptionally flat to meet the critical dimension control and overlay budget requirements. The EUVL Mask Standard, SEMI P37, specifies that the substrate surface nonflatness not exceed 100 nm peak-to-valley (p-v).¹ SEMI P40, the EUVL Mask Chucking Standard, requires the chucking surface nonflatness to be less than 50 nm p-v.² Consequently, EUVL depends upon the capability of an ESC to reduce the final mask nonflatness; the successful implementation of EUVL requires this flattening capability be characterized, predicted, and well understood.

An ESC clamps a substrate to a dielectric chuck surface by electrostatic force. Two types of electrostatic chucks are the Coulomb and Johnsen-Rahbek (J-R),^{3,4} as illustrated in Fig. 1. These are distinguished by the characteristics of their dielectrics and the resulting mechanism of clamping force generation. The Coulomb chuck functions like a conven-

tional dielectric capacitor. The J-R dielectric has a large but finite resistance, so a current flows through it and the substrate when the surfaces are in contact and voltage is applied. Charge accumulates at the interface between the substrate and dielectric. Since the thickness of the interface region is related to surface roughness, the charge separation is typically quite small, and strong electrostatic forces can be generated.

ESCs can have a single electrode or multiple electrodes. If a single voltage is applied to the chuck and the back surface of the mask is electrically grounded, the chuck is monopolar; if voltages of opposite polarity are applied to adjacent electrodes, the chuck is bipolar. The chuck surface can be either flat or covered with elevated pins. Pin chucks are less sensitive to the presence of particles and are preferred for lithography applications, where a flat and undistorted substrate is required.

II. COULOMB STYLE CHUCK

For a monopolar Coulomb chuck, the electrostatic pressure, P , is given by

$$P = \frac{\epsilon_o V_o^2 K^2}{2(t_D + K\delta)^2}, \quad (1)$$

where V_o is the applied voltage, K is the relative permittivity of the dielectric, ϵ_o is the permittivity of free space (8.85

^{a)}Electronic mail: mikkelsen@cae.wisc.edu

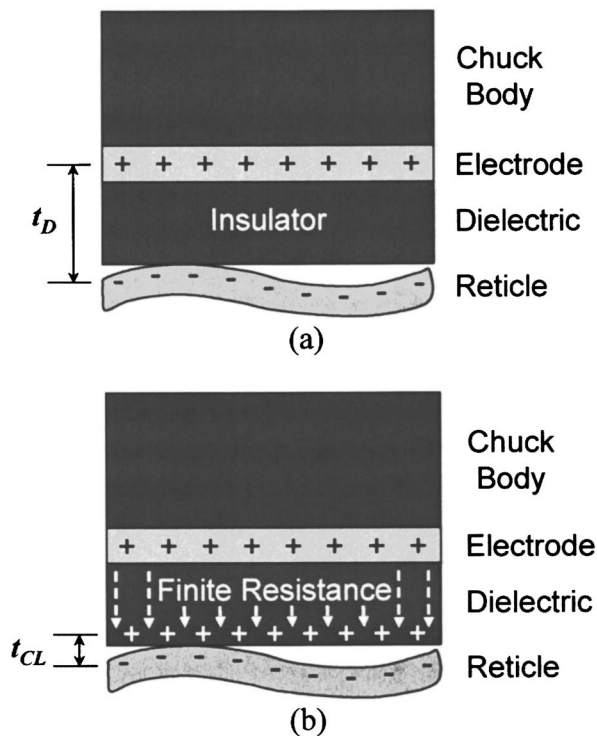


FIG. 1. Schematic of electrostatic force generation in (a) Coulomb and (b) Johnsen-Rahbek chucks.

$\times 10^{-12}$ F/m), t_D is the dielectric thickness, and δ is the total gap between the backside of the mask and the dielectric surface. For a given applied voltage, the pressure generated by a monopolar chuck is four times larger than that from a bipolar chuck. Only monopolar chucks are examined in this paper.

A characteristic of the Coulomb chuck is that clamping pressure exists everywhere between the reticle and chuck. Typical values for t_D in a Coulomb chuck are 100–200 μm and the $K\delta$ term in the denominator of the pressure equation is often an order of magnitude smaller than t_D . Thus, the clamping force is virtually unaffected by the presence of nonflat substrates or entrapped particles (considering relatively small gaps), as illustrated in Fig. 2.

III. JOHNSEN-RAHBK STYLE CHUCK

Details of the clamping characteristics of a J-R chuck are illustrated in Fig. 3(a). When voltage is applied, charge accumulates along the rough chuck-substrate interface or contact layer. This layer has a thickness t_{CL} , which is related to surface roughness, as illustrated in the figure. The properties of the chuck also depend on the resistances of the bulk dielectric (R_V) and the contact layer (R_{CL}). In addition to the attractive force generated in the contact layer, a conventional Coulomb chuck force is also generated between the substrate and the chuck electrode.

While the details of the accumulated charge in the contact layer are quite complicated, a phenomenological model of the J-R chuck force mechanism can be created by treating the contact layer as a small air gap capacitor of thickness t_{CL} .

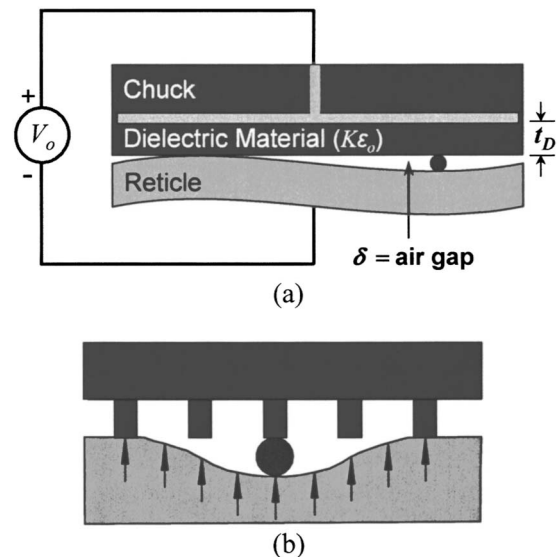


FIG. 2. (a) Characteristics of a Coulomb chuck and (b) corresponding pressure distribution with an entrapped particle.

The amount of charge deposited at the contact layer (or equivalently the voltage drop) can be related to the relative values of R_V and R_{CL} , which function as a resistive divider. This results in the following expression for the clamping pressure, P :

$$P = \frac{\epsilon_0 V_0^2}{2} \left[\left(\frac{K}{t_D + K(\delta + t_{CL})} \right)^2 + \alpha \left(\frac{(R_{CL}/R_V)}{t_{CL}\{1 + (R_{CL}/R_V)\}} \right)^2 \right], \quad (2)$$

where the parameter α is an empirical factor representing the effect of a nonuniform charge distribution on the interface, and δ is now the physical gap between the reticle and dielectric layer. In practice R_V and R_{CL} can be measured; t_{CL} can then be obtained from a measurement of pressure at a given voltage.

The first term in the expression arises from the conventional Coulomb force between the chuck electrode and the substrate. The second term arises from the J-R effect. Typically $t_D \gg t_{CL}$, so the Coulomb term is negligible compared to the J-R term. The empirical factor α represents the effect of the nonuniform distribution of charge on the interface surfaces. Here a value of 2.5 was assumed.⁵

The J-R force depends on electrical contact between the chuck and substrate. This leads to distinctly different behavior from that of the Coulomb chuck when nonflat substrates or particles are present, as illustrated in Fig. 3(b). No J-R clamping force is generated in the noncontacting regions. This brings into question the effectiveness of the J-R chuck for high flatness requirement applications and is a major motivation for the present study.

While relatively high pressures are possible because of the small values of t_{CL} , the effective pressure dependence on voltage changes with increasing voltage. Initially pressure is proportional to the applied voltage squared, as represented in Eq. (2). As the voltage is increased, the interface region com-

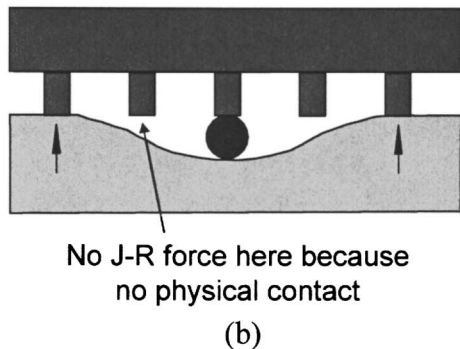
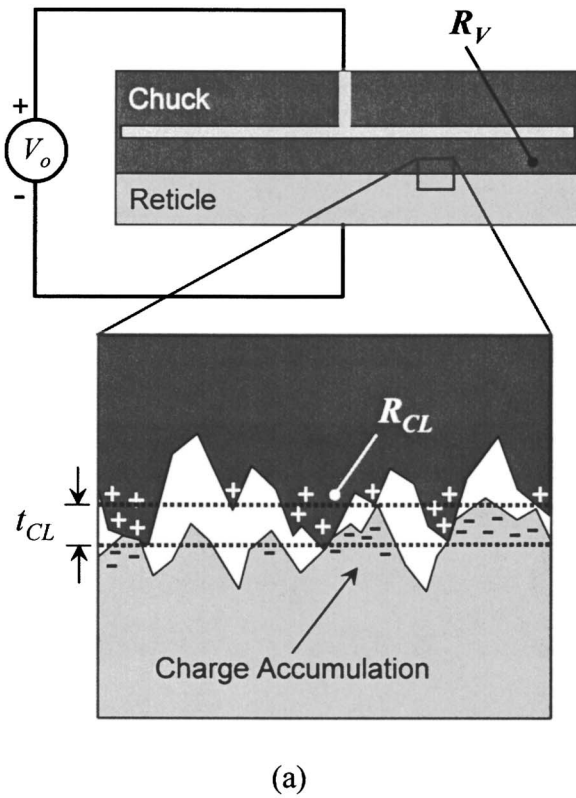


FIG. 3. (a) Characteristics of a J-R chuck and (b) corresponding pressure distribution with an entrapped particle.

presses and the contact area increases, leading to pressures proportional to V_o^n where n is greater than 2. Eventually electron field emission from sharp edges at the interface limits the electric field magnitude. Field emission (in general) may depend on the voltage polarity, since chuck and reticle surfaces may have different work functions and surface roughness.⁶

Finite element (FE) analyses have been used to investigate the J-R performance for nonflat substrates. However, the contact requirement for J-R force generation causes a problem because of the finite mesh of the model. Therefore, for computational convenience a finite range is assumed for the J-R force. The finite range is introduced into Eq. (2) by redefining the constant α as a gap dependent function. As

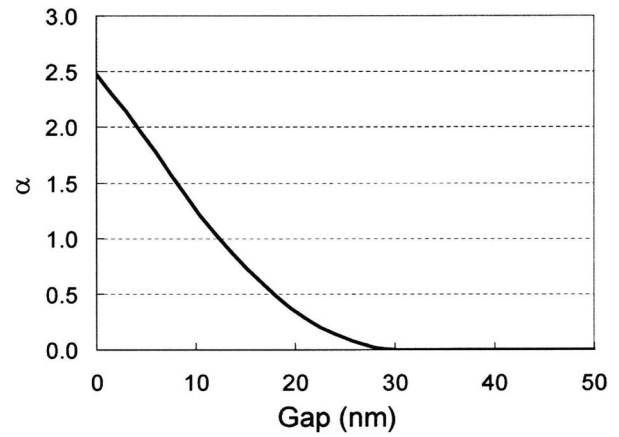


FIG. 4. Relationship assumed for α , a dimensionless empirical factor representing the effect of a nonuniform charge distribution, as a function of gap.

shown in Fig. 4, α , and therefore the J-R force, are defined to be zero at a gap of 30 nm or larger. While this finite range is introduced to facilitate convergence within the FE model, short range forces, such as van der Waals ($\propto 1/\text{gap}^3$) and Casimir ($\propto 1/\text{gap}^4$), exist over a comparable distance⁷ and would be included in a more complete theory.

IV. ELECTROSTATIC PRESSURE DESIGN CURVES

To illustrate the relative importance of the various parameters in the Coulomb and J-R pressure equations, a number of design curves are shown in Fig. 5. The area weighted average pressure (in kPa) has been calculated assuming complete contact between the pins and the backside of the reticle,

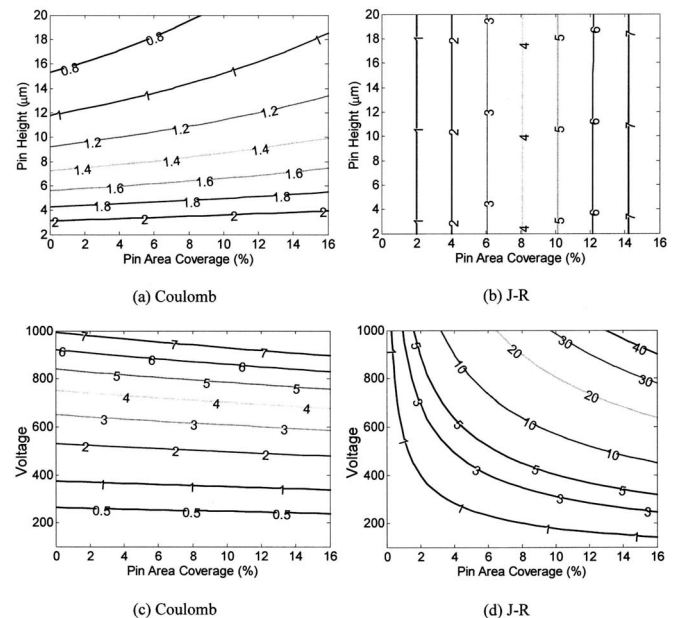


FIG. 5. Design curves illustrating chucking pressure (in kPa) as a function of pin height vs. percent pin area coverage for (a) Coulomb and (b) J-R electrostatic chucks. Design curves illustrating chucking pressure (in kPa) as a function of voltage vs. percent pin area coverage for (c) Coulomb and (d) J-R electrostatic chucks.

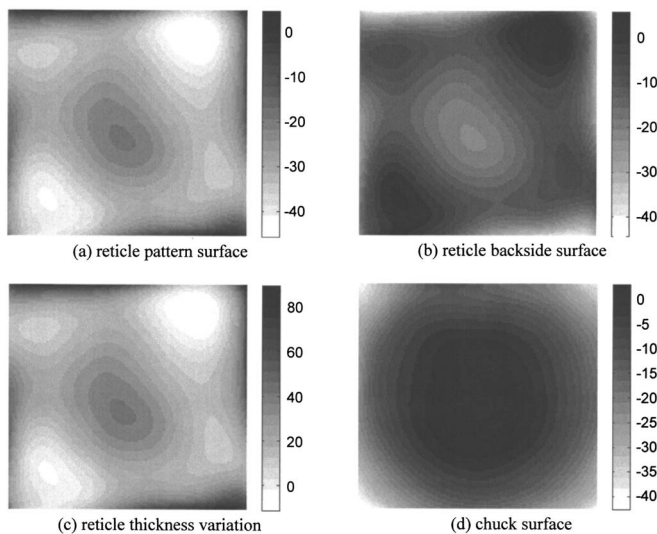


FIG. 6. The mathematical representation of (a) reticle pattern surface (p-v: 50 nm), (b) reticle backside (or chucking) surface (p-v: 50 nm), (c) reticle thickness variation (max: 100 nm), and (d) chuck surface (p-v: 45 nm).

for both types of chucks. Figures 5(a) and 5(b) illustrate the effects of pin height and pin area coverage, respectively, and Figs. 5(c) and 5(d) show the dependence on voltage and pin area coverage. In all cases the relative dielectric constant was assumed to be 10, the dielectric thickness for the Coulomb chuck was 150 μm , and for the J-R chuck the thicknesses of the contact layer and dielectric layer were 1.0 μm and 2.0 mm, respectively. For the J-R chuck, the ratio of the resistance of the contact layer to the volume (or bulk) resistance of the dielectric was assumed to be 0.2. Figures 5(a) and 5(b) assume an applied voltage of 400 V and illustrate that, for a J-R chuck, the pin height has a negligible effect on average pressure for these nominal parameters. Figures 5(c) and 5(d) assume a pin height of 10 μm ; at low values for the pin area coverage, the two styles of chucks generate about the same average pressure. However, as illustrated in both cases, the J-R chuck is able to generate significantly higher average pressures at greater values of pin area coverage.

V. FINITE ELEMENT MODEL

In order to predict the clamping ability of Coulomb and J-R electrostatic chucks, full three-dimensional FE models were developed. Parameters were chosen to be representative for each style of chuck and the initial nonflatness of both surfaces of the reticle and of the pin surface of the chuck were based on interferometric measurements of actual chucks and reticles to provide a realistic and impartial comparison.

The surface of a polished EUVL substrate was measured with a Zygo interferometer. The measured data were scaled to meet the EUVL standard for freestanding reticle flatness and mathematically fitted with Legendre polynomials up to the seventh order. The resulting surface had a p-v of 50 nm and is shown in Fig. 6(a). The Legendre coefficients were

used to define the pattern surface of the substrate in the FE model.

For demonstration purposes, the signs of the Legendre coefficients were switched and used to define the chucking surface of the substrate as shown in Fig. 6(b). With the free-standing p-v of both surfaces at 50 nm, the resulting thickness variation was 100 nm, as shown in Fig. 6(c). Thus, the substrate met the flatness and thickness variation standards set in SEMI P37. In addition, the substrate was assumed to be ULE[®] and of standard size ($152 \times 152 \times 6.35$ mm³).

After defining the initial geometry of the substrate, the deposition of the multilayer was simulated to establish the final configuration of the EUVL reticle. The multilayer was assumed to have uniform thickness and stress that induced a spherical bow of 1.0 μm ; the resulting shape of the reticle pattern surface was convex due to the compressive stress in the multilayer.

The surface of a Coulomb pin chuck was measured and used to represent the chuck surface in the FE model. Again, the surface nonflatness data from the Zygo interferometer were scaled to meet the EUVL chuck standard for flatness and represented with Legendre polynomials; this surface is shown in Fig. 6(d) and has a p-v of 45 nm. These Legendre coefficients were used to define the surface of the pins in the FE model.

The pin chuck was modeled to have a 12×12 array of square pins, each having a side length of 2.5 mm and a height of 10 μm . The pin pitch was 12.67 mm and the coverage was 4%. The pin region was 142 mm² corresponding to the reticle quality area. The chuck was assumed to have an elastic modulus of 380 GPa and a Poisson's ratio of 0.24, which is typical for ceramic materials used in electrostatic chucks. A total thickness of 22.5 mm was used for the body of the chuck, which included a 150 μm thick dielectric for the Coulomb chuck and 2.0 mm thick dielectric for the J-R chuck.

Separate models were developed for each style of chuck and each model included the local gap-dependent pressure. All gravitational effects were ignored, and the coefficient of friction was assumed to be 0.2. The simulations were used to predict the final flatness of the reticle patterned and backside surfaces, the final bow (or flatness) of the chuck, the final gap between the reticle and chuck, and also the pressure distribution on the backside surface of the reticle or the pressure distribution on the pins.

For each model it was assumed that the relative dielectric constant was 10. The model of the Coulomb chuck utilized an applied voltage range of 365 to 895 V, which corresponds to an average pressure (with complete chucking) of 1.0 to 6.0 kPa. The J-R model assumed a contact layer thickness of 1.0 μm and the voltage was varied from 284 to 696 V, which produces an average pressure of 1.0 to 6.0 kPa.

Results from the FE simulations are shown in Fig. 7. The remaining gap for an average pressure of 1.0 kPa is shown in Figs. 7(a) and 7(b) from the Coulomb and J-R models, respectively. In both cases the maximum gap is around 20 nm. For this example case, the models predict that an average

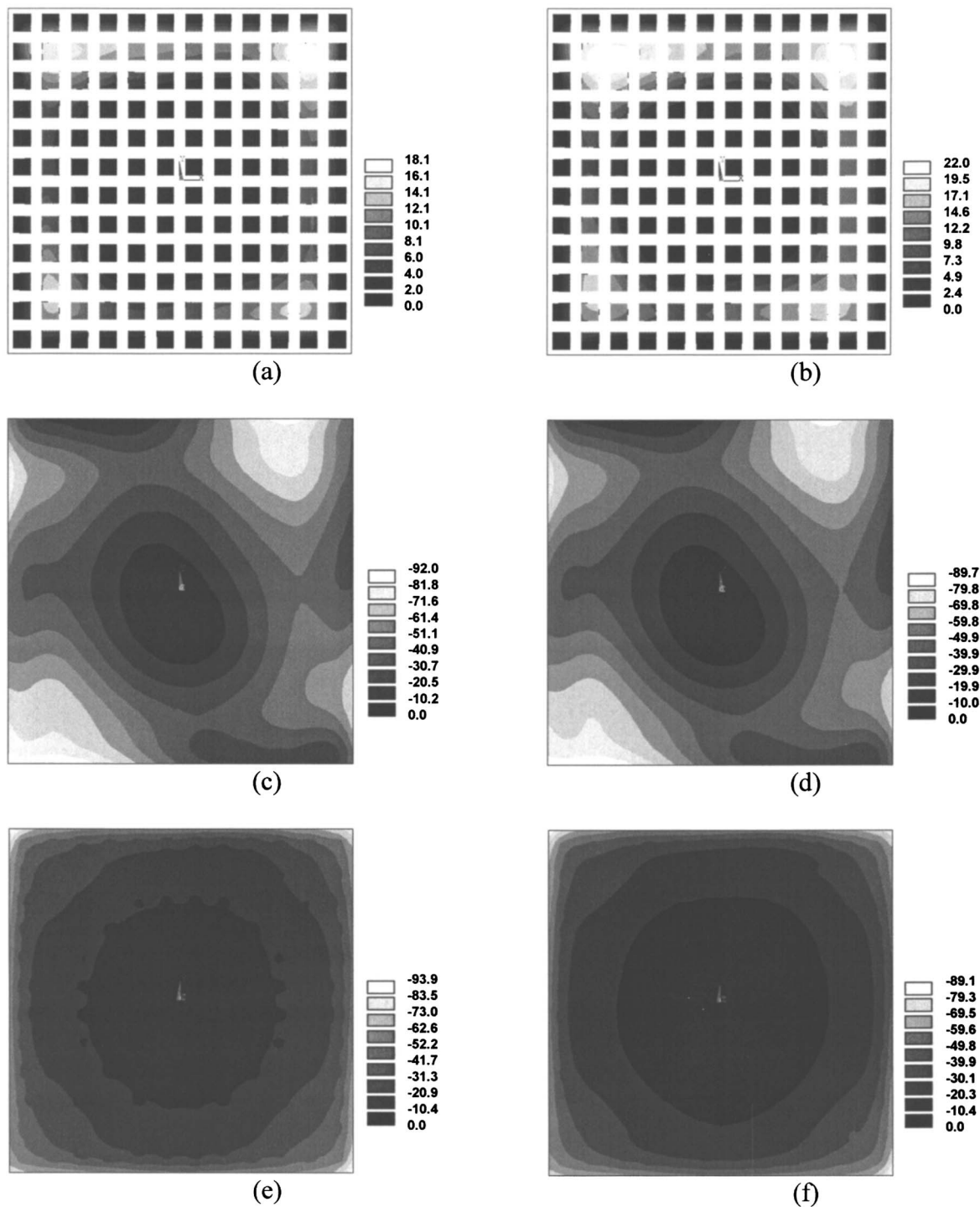


FIG. 7. Summary of FE results. Residual gap at 1 kPa average pressure for (a) the Coulomb chuck and (b) the J-R chuck. Note that the size of the pin areas are exaggerated for display purposes. Reticle pattern surface after chucking with an average pressure of 6.0 kPa on a (c) Coulomb chuck and (d) J-R chuck. Reticle backside surface after chucking with an average pressure of 6.0 kPa on a (e) Coulomb chuck and (f) J-R chuck. All scales are in nanometers.

pressure of 1.0 kPa is sufficient to reduce the gap from an initial value of 1.0 μm down to approximately 20 nm. At an average pressure of 6.0 kPa, the remaining gap is predicted to be negligible.

Figures 7(c) and 7(d) show the final pattern surface shape of the reticle at an average pressure of 6.0 kPa; the shapes are very similar. For these plots the applied voltages for the

Coulomb and J-R cases were 895 and 696 V, respectively. The p-v value for these surfaces is approximately 90 nm, and the p-v value within the quality area for both is just under 80 nm. Since the models predicted almost complete chucking at 1.0 kPa, the pattern surface flatness of the reticles did not change significantly between an applied average pressure of 1.0 and 6.0 kPa.

The final flatness of the backside (or chucking surface) of the reticle is shown in Figs. 7(e) and 7(f) for the Coulomb and J-R models, respectively, for an average pressure of 6.0 kPa. Both models predict the backside surface to have a p-v of about 90 nm and a p-v value of approximately 50 nm within the quality area. The overall shapes of the contours of these plots are quite similar; however, the local distortion at or between the pins is much more apparent in the Coulomb case.

A prediction of the final reticle pattern surface flatness can be generated from the reticle thickness variation and the chuck flatness (without using an FE model). If the chuck were perfectly rigid and the pressure sufficient to produce complete chucking (no residual gap), the pattern surface shape would essentially be equal to the sum of the reticle thickness variation [see Fig. 6(c)] and the chuck surface non-flatness [see Fig. 6(d)]; this sum is shown in Fig. 8(a). The p-v of Fig. 8(a) is 95 nm. The difference between Fig. 8(a) and Figs. 7(c) and 7(d) is due to the nonrigid chuck and the small remaining gap in the FE simulations.

Figure 8(b) is a plot of the remaining gap as a function of average pressure. The Coulomb chuck results in smaller gaps at lower pressure and the J-R chuck provides slightly smaller gaps at larger average pressures. Figure 8(c) is a plot of the pressure as a function of the gap illustrating the pressure both at and between the pins for both chuck types. The data for the plot were generated using the base parameters listed previously in this section and a Coulomb voltage of 365 V and a J-R voltage of 284 V; these voltages correspond to a 1.0 kPa average pressure. The plot shows that the Coulomb pressure is more uniform spatially and over the gap caused by initial nonflatness. Even though the Coulomb and J-R chucks have drastically different pressure dependence on the gap, both are able to completely flatten the reticle against the chuck.

VI. SUMMARY AND CONCLUSIONS

The governing pressure equations for Coulomb and J-R chucks were presented and, for the nominal parameters used, the J-R chuck was capable of producing significantly higher pressures for the same applied voltage in the contact (pin) regions. Due to the J-R chuck dependence on contact to initiate charge accumulation, the J-R chuck pressure is spatially nonuniform and restricted to the contacting regions. However, due to the Coulomb chuck having a spatially uniform pressure distribution, it could cause some reticle distortion between pins. A desirable attribute of a Coulomb chuck is that the pressure is not highly dependent on the gap and therefore would not change appreciably due to the presence of a particle. If relatively tall pins are required to minimize particle effects, the force in a Coulomb chuck could be significantly reduced while the pressure in a J-R chuck would change a negligible amount. However, what still needs to be determined is how a J-R chuck will perform with a particle between a pin and the backside of the reticle. Additionally, in-plane distortion of the reticle surface was not included in this study.

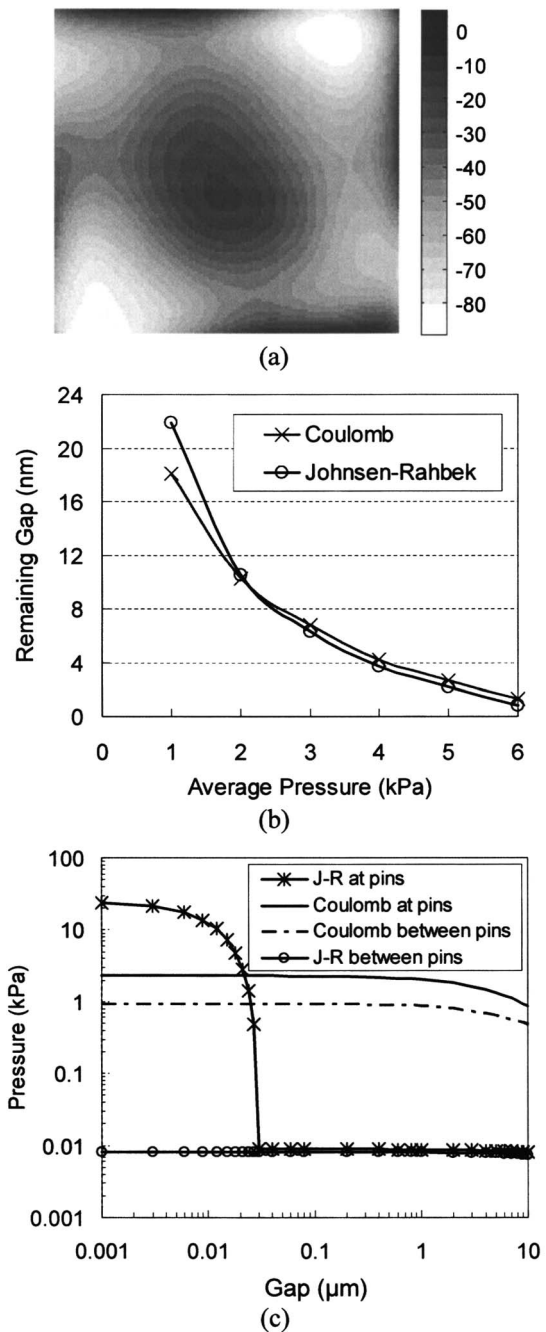


FIG. 8. (a) Prediction of reticle pattern surface flatness from interferometric measurements. (b) Summary of the gap as a function of average pressure. (c) Pressure as a function of gap for the case of an average pressure of 1.0 kPa.

The FE simulations indicated that for the example case considered, average pressure was a good predictor of final gap and flatness regardless of the chuck type. Both styles of chucks were able to pull the nonflat reticle to complete contact with the nonflat chuck with reasonable average chucking pressures. FE simulation results are being used to establish specifications for chuck geometry and to identify the range of flatness variations that can be controlled with electrostatic chucking.

ACKNOWLEDGMENTS

This research has been funded by Nikon, SEMATECH, Intel, and the Semiconductor Research Corporation. Computer support was provided by the Intel Corporation and Microsoft.

¹SEMI P37–1102, SEMI Standard Specification for Extreme Ultraviolet Lithography Mask Substrates.

²SEMI P40–1103, SEMI Standard Specification for Mounting Requirements and Alignment Reference Locations for Extreme Ultraviolet Lithography Masks.

³L. D. Hartsough, *Solid State Technol.* **35**, 87 (1993).

⁴D. Wright, L. Chen, P. Federlin, and K. Forbes, *J. Vac. Sci. Technol. B* **13**, 1910 (1995).

⁵T. Watanabe, T. Kitabayashi, and C. Nakayama, *Jpn. J. Appl. Phys., Part 1* **32**, 864 (1993).

⁶B. Levchenko, arXiv:cond-mat/0512513.

⁷H. B. Chan, V. A. Aksyuk, R. N. Kleiman, D. J. Bishop, and F. Capasso, *Science* **291**, 1941 (2001).